STM/AFM IMAGES AND TUNNELING SPECTRA OF $Nd_{2-x}Ce_xCuO_{4-y}$ SINGLE CRYSTALS

B. Susla[a], W. Sadowski[b], T. Klimczuk[b] and R. Czajka[a]

[a]Institute of Physics, Poznań University of Technology
Piotrowo 3, 60-965 Poznań, Poland
[b]Department of Applied Physics and Mathematics, Technical University of Gdańsk
Narutowicza 11/12, 80-952 Gdańsk, Poland

The results of the scanning tunneling microscopy and spectroscopy as well as atomic force microscopy measurements on the $Nd_{2-x}Ce_xCuO_{4-y}$ single crystals in ambient conditions are reported. Using the scanning tunneling microscopy we were able to modify the $Nd_{2-x}Ce_xCuO_{4-y}$ ab-plane in air under the conditions of sample bias voltage $V_t = 500$ mV and set current $I_s = 0.3$ nA. It is possible to prepare atomically flat and clean surfaces as well as to create new structures in a nanometer scale in these electron-doped materials. The similar processes were not observed during atomic force microscopy imaging.

PACS numbers: 74.72.Jt, 61.16.Ch, 68.35.Bs

1. Introduction

The invention by Tokura et al. [1] of the electron-doped cuprate superconductors, $Nd_{2-x}Ce_xCuO_{4-y}$ (NCCO) with an optimal superconducting transition temperature $T_c = 24$ K at the Ce concentration of $x = 0.15$ is a particularly interesting member of the high-T_c copper oxide superconductor family. Tokura et al. [1] showed that the structure of these compounds is similar to the undoped parent compound Nd_2CuO_4 (T'-phase). The unit cell contains a single CuO_4 plane perpendicular to the c-axis with Nd atoms directly above and below the Cu atom. One of the features of the NCCO is the only electron-doped high-T_c superconductor, in which tetravalent Ce^{4+} ions were doped into trivalent Nd^{3+} ions. This produces charge carriers which are believed to be electrons (n-type doping) rather than holes (p-type) as is the case for the majority of the high-T_c superconductors. Charge carriers in these materials appear to be electrons since both the Hall [2, 3] and Seebeck [2, 4] coefficients were found to be negative. Tranquada et al. [5] show that the electrons introduced by Ce doping are used to fill Cu $3d$ holes to produce Cu^+ ions.

Tunneling spectroscopy is not a new technique and has been used long before the scanning tunneling microscope (STM) was discovered to examine properties

of the tunneling junctions. The development of the atomic resolution scanning tunneling microscopy and spectroscopy (STS) by Binnig and co-workers [6] in 1981 opened a new era of surface science and engineering. Combined STM/STS studies provide useful information about the relationship between atomic surface and local electronic structure.

Since the invention of the atomic force microscope (AFM) by Binnig et al. [7], the surface of poorly conducting substrates or bulk insulators can be investigated on the atomic scale as well. In addition, local mechanical properties can be probed by force microscopy and spectroscopy. In this paper, we present the experimental results of the STM/STS and AFM studies on the $Nd_{2-x}Ce_xCuO_{4-y}$ single crystal in normal state. We observe reproducible STM and AFM images of the surface in air. Spectroscopic data showed that the *ab*-planes of the single crystals NCCO in normal state were semiconductors.

2. Experimental details

The single crystals of $Nd_{2-x}Ce_xCuO_{4-y}$ used in our experiments were grown by a flux technique in alumina crucibles [8]. Unreacted oxides with purity of 99.99%, with the exception of Cu_2O (purity 98%), were mixed in a mass ratio of $Nd_2O_3 : CeO_2 : Cu_2O = 38 : 3 : 59$. This mixture was rapidly heated in air (900°C/h) from room temperature to 1250°C, soaked for 30–60 minutes, then slowly cooled to 1050°C at the rate of 3–5°C/h and finally quenched to room temperature. The atmosphere in the furnace was O_2 at high temperatures (1250–1180°C) and Ar below 1180°C. Black and shiny crystals, mechanically removed from the crucible, had dimensions up to $10 \times 8 \times 0.2$ mm^3. The as-grown $Nd_{2-x}Ce_xCuO_{4-y}$ crystals are semiconductors and the reduction step is required to transform the materials to the superconducting phase. Two nearly identical plate-like crystals were selected for the experiment. The superconductivity was achieved by annealing at 900°C for 15 h in Ar, and then cooling to room temperature over a period of 1 h. The oxygenated (nonsuperconducting) crystal was annealed in O_2 at 900°C for 15 h and then slowly cooled for 10 h to room temperature.

Room-temperature STM/AFM (OMICRON) was used to study the topography and spectroscopic properties of the crystals. The STM images in constant current mode and AFM images in constant force mode were taken immediately after cleaving the single crystals at the room temperature. The tunneling tips were electrochemically etched from 0.25 mm Pt–Ir wire. The voltage applied to the tip ranged from 200 to 2000 mV and tunneling current from 0.2 to 1.0 nA. Commercially available Si_3N_4 cantilevers with integrated tips were used for AFM measurements. Maximum area available to scan was 5×5 μm^2 and typical images consisted of 256×256 lines/points. The scan rate was within range of few Hz per line. The STM/AFM resolution was 0.01 nm in *z*-direction and 0.05 nm in surface plane. The lateral and vertical calibration was realized by imaging the known atomic structure and height of the atomic steps of graphite and mica.

3. Results and discussion

The experiments showed good stability of the $Nd_{2-x}Ce_xCuO_{4-y}$ surface and possibility to observe reproducible AFM images of the fresh surface in air. Figure 1 presents an AFM atomic image of $4 \times 4 nm^2$ area with the 0.2 nm corrugation for reduced in Ar single crystals. The STM atomic image at 300 K for reduced NCCO crystal was also observed, indicating an electronic modulation longer than the *b*-direction lattice constant [9]. Figure 2a shows AFM top-view image of 2000×2000 nm^2 surface for the same sample as in Fig. 1, which indicates stepped structures of a few hundred nanometers width and some spiral-type structures at step edges. Topography measurements with higher magnification in the vertical direction (Fig. 2b) showed the existence of growth spirals. The height of these structures was higher than the *c* parameter of the unit cell of NCCO. We did not observe any changes on the examined NCCO surface with changing the AFM experimental parameters e.g., force set-point. However, for oxygenated NCCO crystals we observed regular higher corrugations of planar structure as shown in Fig. 3, where typical values were 10–40 nm randomly distributed throughout the sample surface.

Using the STM we were able to modify the NCCO *ab*-plane in air under the conditions of sample bias voltage $V_t = 500$ mV and set current $I_s = 0.3$ nA. This process may be explained in terms of evaporation of a surface layer (e.g. oxides) present on the top of NCCO sample, due to the presence of a high electric field of 10^9 V/m [10]. The similar processes were not observed during AFM imaging.
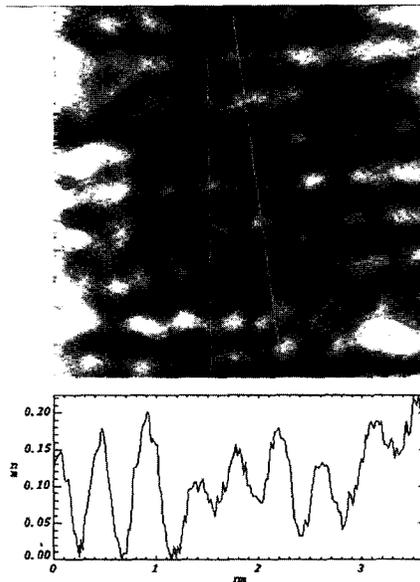
Fig. 1. AFM 4×4 nm^2 top-view image of reduced $Nd_{2-x}Ce_xCuO_{4-y}$ surface taken at 300 K and a cross-line section along the line marked on the top-view image.
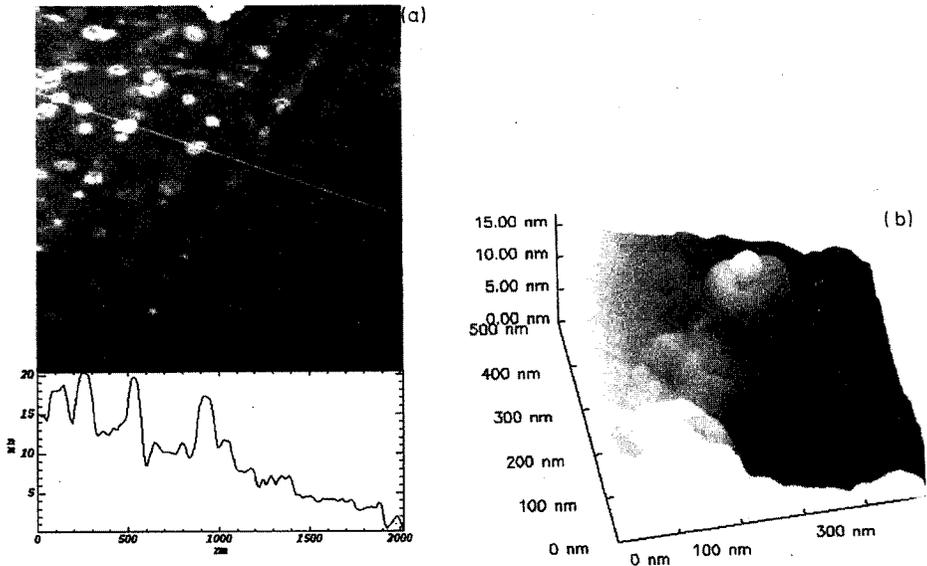
Fig. 2. (a) AFM 2000 × 2000 nm^2 image of the reduced Nd$_{2-x}$Ce$_x$CuO$_{4-y}$ surface taken at 300 K and a cross-line section along the line marked on the top-view image. (b) Higher magnification of individual step region with a growth spiral-type structures — AFM 500 × 500 nm^2 (3D) image.
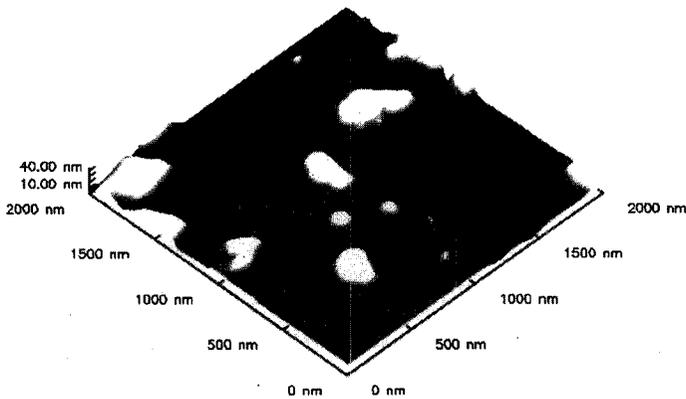
Fig. 3. AFM 2000 × 2000 nm^2 (3D) image of oxygenated Nd$_{2-x}$Ce$_x$CuO$_{4-y}$ sample surface.

Figure 4 shows STM image of 1000 × 1000 nm^2 of oxygenated sample which indicates a regular stepped structure. In this picture the height of each step corresponds within the experimental error to a height of a few unit cells in the c direction. The cross-line section along the line marked on the top-view image reveals the step with a height that is an integer factor of the lattice constant ($c = 1.2$ nm). As one can observe on the cross-line section (Fig. 4), there
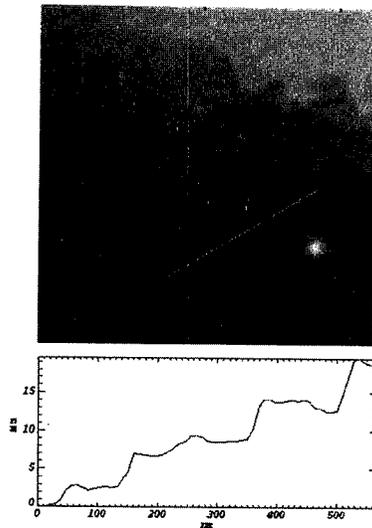
Fig. 4.   STM 1000×1000 nm^2 image of oxygenated Nd$_{2-x}$Ce$_x$CuO$_{4-y}$ sample surface and a cross-line section along the line marked on the top-view image.
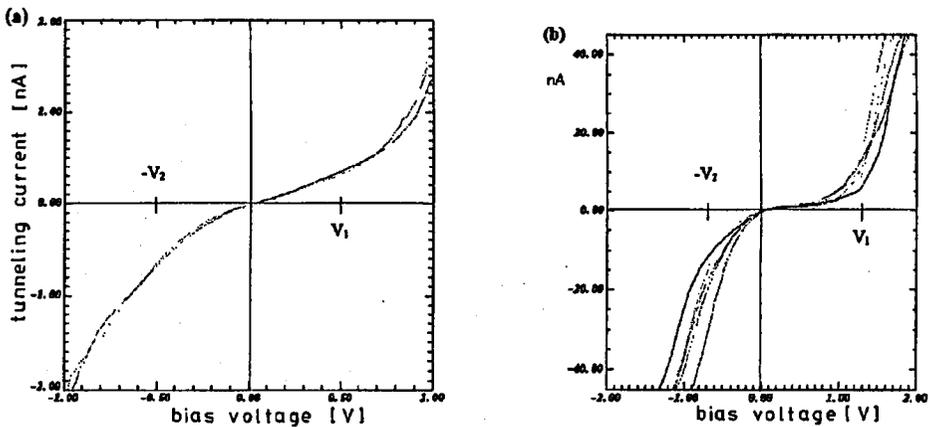
Fig. 5.   Tunneling current versus voltage curves for oxygenated (a) and reduced (b) Nd$_{2-x}$Ce$_x$CuO$_{4-y}$ sample taken at different spots on the surface.

are sectors of one hundred nanometers length with corrugations less than one c lattice constant.

We also performed scanning tunneling spectroscopy measurement of the local $I-V$ characteristics. We found that the $I-V$ curves are generally of two types depending on the oxygenated and reduced crystals of Nd$_{2-x}$Ce$_x$CuO$_{4-y}$. They exhibit characteristic semiconductor features at room temperature. The semicon-

ducting gap is $E_g \approx 1.0\,\mathrm{eV}$ for oxygenated single crystals (Fig. 5a) and $E_g \approx 2.0\,\mathrm{eV}$ for reduced $Nd_{2-x}Ce_xCuO_{4-y}$ crystals (Fig. 5b). The energy gap of the semiconductor, E_g, in normal state for NCCO single crystals, is expressed in the following equation: $E_g = |V_1| + |V_2|$. As shown in Figs. 5a and 5b both the $I-V$ characteristics are nonlinear but the voltages V_1 and V_2, at which the currents start to steeply increase or decrease, are different depending on the sample preparation (reduced or oxygenated). From Fig. 5a V_1 and V_2 are about 0.5 V and 0.5 V respectively, so that E_g is estimated to be (1.0 ± 0.1) V. Figure 5b shows V_1 and V_2 which are about 1.3 V and 0.7 V, respectively, so that E_g is (2.0 ± 0.1) V. Tunneling electron spectroscopy of NCCO was studied by using STM in order to obtain insight into the electronic energy structure of the electron-doped superconductor.

4. Conclusions

The relation between the microstructure of the crystals and the used growth technique were studied using room-temperature STM/AFM. Using the STM, we were able to modify the NCCO surface in air. It is possible to prepare atomically flat surface and create new structures in these electron-doped materials. From $I-V$ characteristics we could estimate the width of a semiconducting gap of reduced and oxygenated single crystals.

Acknowledgments

References

[1] Y. Tokura, H. Takagi, S. Uchida, *Nature* **337**, 345 (1989).

[2] H. Takagi, S. Uchida, Y. Tokura, *Phys. Rev. Lett.* **62**, 1197 (1989).

[3] W. Sadowski, M. Affronte, E. Walker, T. Klimczuk, B. Kusz, M. Gazda, M. Luszczek, O. Gzowski, *Mol. Phys. Rep.* **12**, 213 (1995).

[4] S. Uchida, H. Takagi, H. Ishi, H. Eisaki, T. Yabe, S. Tajima, S. Tanaka, *Jpn. J. Appl. Phys.* **26**, L440 (1987).

[5] J.M. Tranquada, S.H. Heald, A.R. Moodenbaugh, G. Liang, M. Croft, *Nature* **337**, 720 (1989).

[6] G. Binnig, H. Rohrer, Ch. Gerber, E. Weibel, *Appl. Phys. Lett.* **40**, 178 (1982).

[7] G. Binnig, C.F. Quate, Ch. Gerber, *Phys. Rev. Lett.* **56**, 930 (1986).

[8] W. Sadowski, H. Hagemann, M. Francois, E. Walker, *Physica C* **170**, 103 (1990).

[9] B. Susła, R. Czajka, W. Sadowski, T. Klimczuk, *Mol. Phys. Rep.*, in preparation.

[10] B. Susła, R. Czajka, W.S. Gordon, S. Szuba, J. Raułuszkiewicz, *Mater. Sci. Eng. A* **217/218**, 419 (1996).